Nuclear Physics B(97) (1975) 189–200

SEARCH FOR STABLE PARTICLES OF CHARGE ⩾ 1 AND MASS ⩾ DEUTERON MASS

M.G. ALBROW, D.P. BARBER, P. BENZ, B. BOŠNJAKOVIĆ, J.R. BROOKS, C.Y. CHANG *, A.B. CLEGG, F.C. ERNÉ, P. KOOIJMAN, F.K. LOEBINGER, N.A. McCUBBIN, P.G. MURPHY, A. RUDGE, J.C. SENS, A.L. SESSOMS **, J. SINGH and J. TIMMER

CERN, Geneva, Switzerland
Daresbury Laboratory, UK
Foundation for Fundamental Research on Matter, (FOM), The Netherlands
University of Lancaster, UK
University of Manchester, UK
University of Utrecht, The Netherlands

(CHLM Collaboration)

Received 17 June 1975

In a search for stable massive particles of charge $q \geqslant 1$ at the CERN ISR ($\sqrt{s}$ = 53 GeV) no new particle in the mass range $q \times 2.4$ GeV $< m \lesssim 30$ GeV has been found among 3.1×10^7 recorded secondaries. At $x = 2p_L/\sqrt{s} = 0.21$ and $p_T = 0.21$ GeV/c the deuteron to π^+ ratio is $(1.3 \pm 0.2) \times 10^{-4}$ and the antideuteron to π^- ratio is $(7.6 \pm 2.3) \times 10^{-6}$. For (anti)tritons upper limits of $(t/\pi^+) < 5 \times 10^{-7}$ and $(\bar{t}/\pi^-) < 5 \times 10^{-7}$ have been obtained.

1. Introduction

Experiments on the production of massive particles in high-energy pp and p nucleus collisions have been performed at the CERN PS [1,2], Serpukhov [3], NAL [4 –6] and at the ISR [7–9]. Most of these experiments have emphasized the search for fractionally charged particles. No events have been found, yielding upper limits for the total production cross section of 10^{-37} to 10^{-35} cm^2 for quark masses less than 5 GeV/c^2 and 3×10^{-33} to 10^{-31} cm^2 for masses between 5 and 25 GeV/c^2. On the other hand quark schemes with four or more quarks (see for instance refs. [10–13]) suggest the possibility that there exist new families of massive, integrally charged particles with stable ground states. In this paper we present results of a search for heavy stable particles of charge q, with $|q| \geqslant 1$, inclusively

* Present address: University of Maryland, College Park, Maryland 20742, USA.
** Present address: Harvard University, Cambridge, Mass., 02138, USA.

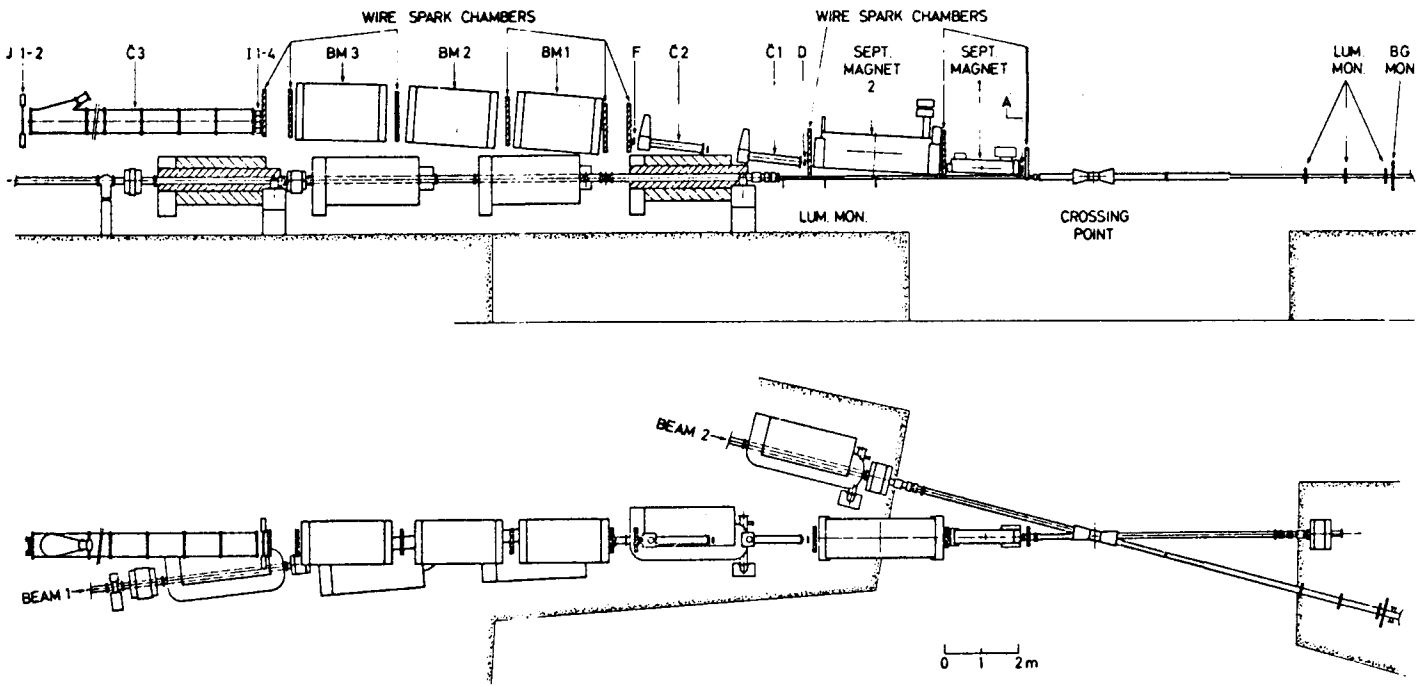

Fig. 1. Side and top views of the small angle spectrometer (SAS), located above the ISR beam 1. BM 1,2,3 are bending magnets, LUM MON is a set of counters for measuring the ISR luminosity. BG MON is a set of counters used to distinguish beam/beam from beam/gas events (see text).

produced at small angles to the direction of two colliding proton beams of 26.7 GeV/c momentum at the CERN ISR. This study was motivated by the possibility that new massive particles, like the known particles, are produced predominantly as the fragments of one of the protons excited in the collision.

2. Apparatus and experimental procedure

The apparatus consists of a small angle single arm spectrometer (SAS) (see fig. 1; for a more detailed description of the SAS see ref. [14]) mounted on top of the CERN ISR beam 1. The SAS acceptance is approximately 6×10^{-4} GeV/c · sr. The particle trajectories were reconstructed by means of nine spark chamber modules with magnetostrictive read-out. The particle masses were calculated from their time of flight (TOF), measured over a total flight path of 27.5 m, and from their momenta determined by five bending magnets. The experiment was performed at a total energy of $\sqrt{s} = 53$ GeV. The spectrometer was set for optimum acceptance of particles with production angles θ between 30 and 50 mrad and momenta p in the range $q \times 4$ to $q \times 10$ GeV/c.

High-mass particles were identified by the following criteria:

(i) A five fold coincidence of the counters A, D, F, I and J (see fig. 1) with signals arranged to accept particles with a velocity $\beta \geqslant 0.28$.

(ii) None of three threshold gas Čerenkov counters C_1, C_2, C_3 (see fig. 1) counted. Counters C_1 and C_2 were filled with ethylene at 30.5 atm pressure and counted particles with $\beta \geqslant 0.976$. Counter C_3, filled with hydrogen at 5.5 atm, counted pions only ($\beta \geqslant 0.9993$). For the accepted range of momenta, protons with $p \gtrsim 4.2$ GeV/c and all kaons and pions were thus vetoed. Light particles leaking through this hardware veto were removed in the software with the aid of the Čerenkov pulse heights.

With this trigger the apparatus was sensitive to particles of masses and momenta in the range shown in fig. 2 (for unit charge). The yield of light particles was determined in short separate runs with criterion (ii) switched off. In these runs pions were uniquely identified by the requirement that all three Čerenkovs had counted.

Data were taken both for positive and negative charges. 1.81×10^7 positive and 1.26×10^7 negative particles, produced in 3.4×10^{10} and 6.3×10^{10} inelastic pp interactions respectively, passed through the spectrometer in the course of the experiment. For triggers fulfilling the above criteria the particle momentum and production angle were determined from the last three bending magnets and the last six spark chamber modules of the spectrometer (see fig. 1). For 97% of these triggers the particle momentum could thus be determined. The fraction of triggers, for which a track within all aperture limits of the spectrometer was found, ranged between 40% and 65% depending on the momentum. 7363 positive and 797 negative particles survived all reconstruction criteria.

For each event we have recorded seven times of flight between the following

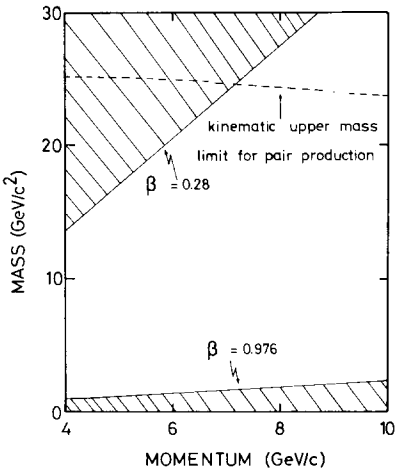

Fig. 2. Mass acceptance as a function of momentum (for unit charge). The dashed line shows the kinematic upper limit for pair production of massive particles for $\sqrt{s}$ = 53 GeV. Events in the shaded area are rejected by the trigger.

four counter pairs: A/F, F/I′, F/J and D/I, where I′ is a four counter hodoscope near the position of I. The TOF measurements have time resolutions between 0.5 and 1 nsec (one standard deviation). Each of the counters A, F, I′ and J is viewed by two independent phototubes, thus providing two independent TOF measurements for each of the first three counter pairs. To reduce tails in the TOF distributions due to false triggers and pulse height fluctuations in the tubes, TOF measurements provided by the same counter pair were required to be compatible. Events with less than 3 TOF measurements surviving this consistency check were rejected (~4%). After correcting for the particle position in the scintillator, for each accepted TOF measurement a value β_i for the particle velocity was calculated from $\beta_i = 1/(1 + c\Delta t_i/L_i)$, where L_i is the corresponding flight path, c is the velocity of light and $\Delta t_i = t_{i,\beta} - \langle t_{i,\beta=1} \rangle$ is the difference of the flight time between the observed particle and a particle with $\beta = 1$. The $\langle t_{i,\beta=1} \rangle$ values were determined from the TOF distributions of pions. The particle mass was then calculated from $(m/q)^2 = (p/q)^2(1/\beta^2 - 1)$, where β is the weighted average of the β_i values, q the particle charge and (p/q) the measured magnetic rigidity.

3. Production of deuterons and antideuterons

The $(m/q)^2$ distributions for positive and negative particles are shown in figs. 3a and b respectively. For momenta $p > q \times 4.2$ GeV/c where (anti)protons are vetoed by trigger criterion (ii) (see above), clear signals at the position of the deuteron mass

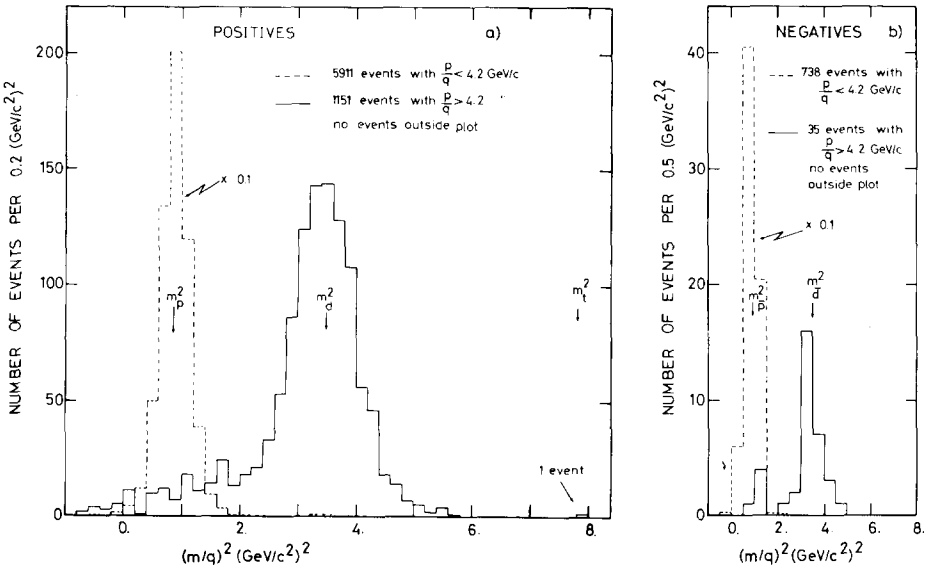

Fig. 3. (a) Distribution of $(m/q)^2$ for positive particles with $(p/q) < 4.2$ GeV/c (dashed lines) and $(p/q) >$ GeV/c (full lines). m is the particle mass and q its charge per electron charge. (b) Same as (a) for negative particles.

squared (3.52 (GeV/c^2)^2) show up in both charge states. The width of the deuteron peak is 1.2 (GeV/c^2)^2 (FWHM) and is consistent with that of the proton peak (0.6 (GeV/c^2)^2), taking into account that the mass resolution is limited by the TOF resolution, i.e. $\delta m^2 = 2p^2\,\delta\beta/\beta^3$, and that $\langle p_p \rangle = 4$ GeV/c and $\langle p_d \rangle = 6$ GeV/c. In the momentum range 4.2 to 8.0 GeV/c 1040 positive (30 negative) particles with $(m/q)^2 > 2$(GeV/c^2)^2 were therefore identified as deuterons (antideuterons).

For the calculation of cross sections one has to take account of possible background events from beam-gas collisions or secondary interactions in the material between the intersection and the first Čerenkov counter (3.5 g/cm^2). A large contamination of the observed deuteron sample due to these effects was found in a previous ISR experiment [8]. Accordingly we have made the following checks:

(i) For each event the flight time difference Δt was recorded between the counter A and a small angle monitor hodoscope [14] surrounding the beam pipe at a distance of 7.7 m from the intersection at the opposite side of SAS with a solid angular acceptance of 0.01 sr (indicated by BG in fig. 1). Sixty-six percent of all deuteron events were in coincidence with a count in this hodoscope and had a Δt within the correct time interval required for an event to be produced in a beam-beam collision. The contamination of the observed deuteron sample by beamgas events was then estimated by comparing the spatial distribution of the reconstructed deuteron track origins for events with and without Δt in the correct interval. We found the contamination to be (1 ± 7)%.

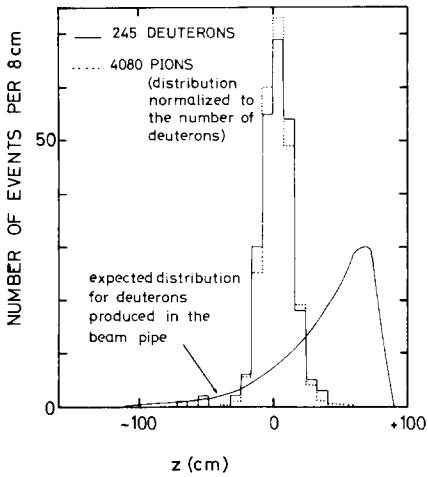

Fig. 4. Distribution of track origins along the beam 1 direction z for deuterons (full line) and pions (dotted line). The full curve shows the expected distribution for deuterons produced in the steel window of the beam pipe (see text), normalized to the number of observed deuterons.

(ii) If a considerable fraction of the observed deuterons was produced by secondary interactions, one would expect the spatial distribution of the deuteron event vertices to be smeared out in comparison with that of light particles, for which this contamination is expected to be small. Fig. 4 shows the distribution of the track origins along the beam 1 direction z for deuterons and pions. The distributions are compatible, i.e. no smearing is observed. To check this point further we have generated by Monte Carlo a sample of primary particles at the centre of the beam crossing region with an angular dependence equal to that observed for high momentum protons [15] and allowed them to produce deuterons in a secondary interaction. The point nearest to the intersection where they can produce deuterons is a 1 mm thick stainless steel window in the beam pipe at 1.6 m downstream of the intersection. For the laboratory differential cross section of deuteron production the form $d^3\sigma/dp d\Omega \sim p^2/E \exp(-ap_T)$ was used. This form, with a slope $a = 4(\mathrm{GeV}/c)^{-1}$, is suggested by available data on deuteron production in p nucleus collisions at PS energies [16–21]. For secondary deuterons accepted by the spectrometer the spurious vertex position was calculated. The resulting z-distribution is shown in fig. 4 (full curve), normalized to the number of observed deuterons. No events are seen in the z-range where the predicted distribution peaks. From this and from order of magnitude estimates of the contamination we conclude that at most a few percent of the observed deuterons are due to proton-nucleus collisions.

The same conclusions apply to the antideuterons, where in addition the question of contamination is less critical due to the high threshold energy for production (16 GeV on stationary nucleons).

Table 1
Deuteron-pion production ratios and invariant cross sections for d and $\bar{d}$ production

x	P_T (GeV/c)	(d/π^+) (10^{-4})	$\sigma_{inv}(d)$ (μb/GeV^2/c^3)	$(\bar{d}/\pi^-)$ (10^{-6})	$\sigma_{inv}(\bar{d})$ (μb/GeV^2/c^3)	$(\bar{d}/d)$ (10^{-2})	$\frac{(\bar{d}/\pi^-)}{(\bar{p}/\pi^-)^2}$ (10^{-3})	$(\bar{p}/p)^2_{\frac{1}{2}p_d}$ [a] (10^{-2})	$\sigma_{inv}(\bar{d})$ predicted by thermod. model (μb/GeV^2/c^3)
0.18	0.16	1.1 ± 0.2	2.0 ± 0.5	7.4 ± 2.7	0.068 ± 0.027	3.4 ± 1.6	9.4 ± 4.0	10.0 ± 3.0	0.048
0.21	0.21	1.3 ± 0.2	1.8 ± 0.4	7.6 ± 2.3	0.056 ± 0.019	3.1 ± 1.2	10.4 ± 3.9	6.3 ± 2.0	0.035
0.25	0.30	2.4 ± 0.4	1.8 ± 0.4	3.4 ± 1.5	0.014 ± 0.006	0.8 ± 0.4	5.3 ± 2.6	3.6 ± 1.0	0.020

[a] Interpolated from refs. [14, 23, 24].

Table 2
$(\bar{d}/d)$ and $(\bar{p}/p)^2$ ratios from various experiments

p_{inc}(GeV/c)	Target	$\langle x_d \rangle$	$\langle p_T \rangle$ (GeV/c)	$(\bar{d}/d)$	$(\bar{p}/p)^2_{\frac{1}{2}p_d}$	Ref.
30	Be	−0.2	0.4	4×10^{-5}	12×10^{-5}	[22, 25]
300	W	0.01	(0°)	4×10^{-2}	25×10^{-2}	[5, 26]
1500	p	~0.02	~0.7	3×10^{-1}	2×10^{-1}	[8, 23]
1500	p	0.2	0.2	2×10^{-2}	6×10^{-2}	this exp. (mean value) and refs. [14, 23, 24]

The cross sections for deuteron and antideuteron production were calculated from the measured d/π ratios using the published cross sections for pion production [14]. Corrections were applied for absorption and decay of the pions as well as for

Table 3
Negative particle ratios from various experiments

p_{inc} (GeV/c)	Target	p_{lab} (GeV/c)	$\langle x_{\bar{d}} \rangle$	$\langle p_T \rangle$ (GeV/c)	$(\bar{d}/\pi^-)$ (10^{-6})	$(\bar{d}/\bar{p})$ (10^{-4})	$\frac{(\bar{d}/\pi^-)}{(\bar{p}/\pi^-)^2}$ (10^{-3})	Ref.
30	Be	5	−0.20	0.4	0.055	0.1	1.5	[22,25]
43	Al	15.5	0.24	(0°)	0.20	0.22	2.4	[28]
70	Al	13.3	0.03	0.6	3.9	1.2	3.4	[29]
		25.1	0.28	(0°)	0.60	0.54	4.9	[28]
		25.1	0.28	0.3	0.79	0.56	4.0	
		39.1	0.51	(0°)	0.05	0.18	6.5	
300	W	24.5	0.01	(0°)	4	2.0	10.0	[5]
		34.2	0.06	(0°)	11	2.8	6.9	
	Be	80	0.24	0.2	2.4	1.2	6.0	[6]
1500	p		0.02	0.7	50	5.0	5.0	[8]
			0.2	0.2	7.6	2.8	7.9	this exp. (mean value)

absorption of the deuterons. In these corrections we assumed $\sigma_{\bar{d}}^{\pm}(p_{lab}) \approx 2\sigma_{\bar{p}}^{\pm}(\frac{1}{2}p_{lab})$ for the absorption cross section; the correction factors are 1.92 for the d and between 2.54 and 2.72 for the $\bar{d}$. A further correction factor of 1.12 was applied to account for losses of deuterons which produce a δ-ray causing a Čerenkov count. This correction was determined from separate runs where only those triggers were vetoed in which more than one Čerenkov counted. Losses due to multiple scattering were assumed to be approximately the same for deuterons and pions (the velocity of a 6 GeV/c deuteron is 0.95 c). The resulting invariant cross sections $\sigma_{inv} = E d^3\sigma/dp^3$ are listed in table 1 for various values of $x = 2p_L/\sqrt{s}$ and p_T. The uncertainties of the various experimental corrections sum up to a total systematic error of ±20%, which is included in the errors given in table 1.

The invariant deuteron cross section shows no strong variation over the accepted x and p_T range whereas the antideuteron cross section decreases with increasing x and p_T. The x and p_T dependence of the $(\bar{d}/d)$ ratio can be understood qualitatively in a model of Dorfan et al. [22] in which two nucelons (antinucleons) are produced independently in the interaction and form a d ($\bar{d}$) when their wave functions overlap. The authors obtain the relation $(\bar{d}/d) \approx (\bar{p}/p)^2$, where the $(\bar{p}/p)$ ratio has to be taken at half of the outgoing deuteron momentum. Table 1 shows the measured $(\bar{d}/d)$ ratios and the corresponding $(\bar{p}/p)^2$ ratios, which were interpolated from the data of refs. [14, 23, 24]. Apart from a scale factor of about 3 the above relation apparently predicts the right shape for the x and p_T dependence of the $(\bar{d}/d)$ ratio. Since in the kinematic region covered in our experiment p and $\bar{p}$ production have essentially the same p_T dependence [14, 23, 24], the different behaviour of the $\bar{d}$ and d cross sections is thus the consequence of the different x dependence of protons ("leading particles") and antiprotons ("fragments"). Table 2 shows the $(\bar{d}/d)$ ratios from various experiments; the corresponding $(\bar{p}/p)^2$ ratios are taken from refs. [25, 26] (thermodynamical model prediction) and [23]. The above relation gives the right order of magnitude for the $(\bar{d}/d)$ ratio from 30 GeV/c incident momentum up to ISR energies.

Antideuteron production has been observed previously at the CERN PS [27], the AGS [22], at Serpukhov [28, 29], NAL [5, 6] and the ISR [8]. Table 3 gives some results for particle production ratios from these measurements. It is difficult to compare these results directly, because the experiments were performed at different production angles and momenta and used different target material. However, it is interesting that all these data can be related by a scaling law [8] for the ratio $(\bar{d}/\pi^-)/(\bar{p}/\pi^-)^2$, although the $(\bar{d}/\pi^-)$ ratio itself varies by more than two orders of magnitude (see table 3). The prediction of the weak bootstrap thermodynamical model [26] for the invariant $\bar{d}$ cross section is given in the last column of table 1; the agreement with the data is reasonable.

4. Production of tritons and antitritons

Among the positive triggers six events with particle masses $> q \times 2.4$ GeV/c^2 survived the analysis procedure. By a careful investigation of the spark locations and

by consistency checks on the momentum determined from the bending in different parts of the spectrometer, five events could be identified as scatters or interactions inside the spectrometer. One candidate was left having $(m/q) = (2.80 \pm 0.12)$ GeV/c^2, $(p/q) = 6.9$ GeV/c and a production angle of 51 mrad. The possibility that this event is a triton produced in a beam-beam collision ($m_t = 2.81$ GeV/c^2) gives an upper limit for the production ratio $(t/\pi^+) < 5 \times 10^{-7}$ with 90% confidence level.

No antitriton was observed, corresponding to an upper limit on the production ratio $(\bar{t}/\pi^-) < 5 \times 10^{-7}$ with 90% c.l. At Serpukhov energies [28] an upper limit of $(\bar{t}/\pi^-) < 10^{-9}$ was found. If one assumes that for $\bar{t}$ production an analogous scaling law is valid, as for $\bar{d}$ production, i.e. that the ratio $(\bar{t}/\pi^-)/(\bar{p}/\pi^-)^3$ scales, one predicts from the Serpukhov result an upper limit of $(\bar{t}/\pi^-) < 7 \times 10^{-9}$ for the kinematic range covered in our experiment.

5. Production of new particles

No new particles of either charge with $m/q > 2.4$ GeV/c^2 (apart from the one triton mentioned above) were observed within the mass and momentum limits shown in fig. 2. This corresponds to the upper limits (90% c.l.) on the non-invariant differential production cross section $d^3\sigma/dp d\Omega$ in the c.m. shown in fig. 5 as a function of the mass m for various particle charges q. The full (dashed) curves are obtained by taking account of the kinematic limits for pair (single) production of massive particles. The mean production angle accepted by the spectrometer is 40 mrad and the mean momentum is $q \times 6.5$ GeV/c, except for $q = 1$ and $m > 15$ GeV/c^2 where it increases from 6.5 GeV/c at $m = 15$ GeV/c^2 to 9.5 GeV/c at $m = 32$ GeV/c^2. In fig. 5 the positive and negative particle data are combined. The upper cross-section limits obtained for positive (negative) particles alone are higher by a factor 3(1.5). The upper limits are not corrected for possible losses in the detector (absorption etc; the total amount of material between the intersection and the end of the spectrometer is 25.5 g/cm^2).

For an estimate of the upper limit on the total cross section for pair production of massive particles two different assumptions have been used:

(i) The invariant cross section has the form $\sigma_{inv} = \text{const.} \times \exp(-a p_T)$ ("leading particle like"). For the slope a values between 2 and 4 (GeV/c)$^{-1}$ are suggested by the data on deuteron production at PS energies [16–21] and antideuteron production at the ISR [8].

(ii) The invariant cross section has the same x and p_T dependence as that for pions ("fragment like"). The x and p_T dependence of pion production was obtained from fits to the contour plots given in ref. [30].

For either assumption the resulting upper limits on the total cross section range between 1 and 10 nb depending on the particle mass (up to 24 GeV/c^2) and charge (between 1 and 2). It may be noted that these limits depend strongly on the assumption that the production cross section for massive particles peaks in the for-

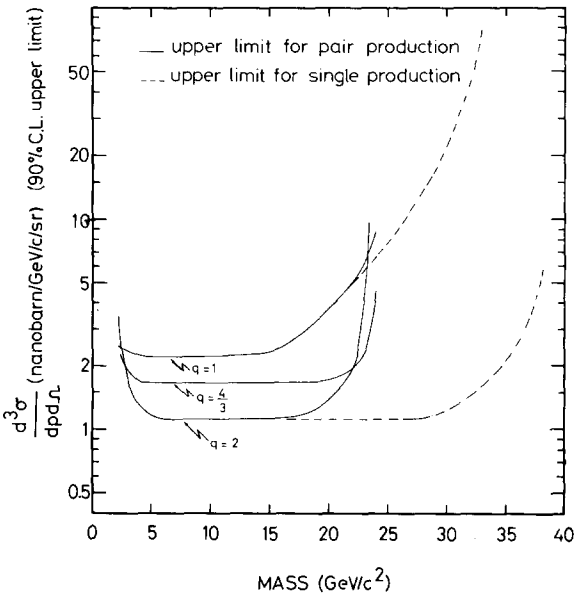

Fig. 5. Upper limits (90% confidence level) on the c.m. non-invariant differential cross section $d^3\sigma/dpd\Omega$ for pair (full curves) and single (dashed curves) production of massive particles as a function of the mass m for various particle charges q. $\langle\theta^*\rangle = 40$ mrad, $\langle p\rangle = q \times 6.5$ GeV/c, except for $q = 1$ and $m > 15$ GeV/c^2 where it increases from 6.5 GeV/c at $m = 15$ GeV/c^2 to 9.5 GeV/c at $m = 32$ GeV/c^2. The limits are not corrected for possible losses of particles in the detector.

ward direction. A comparison with total cross-section limits set by other experiments [4,8,9] (between 3 and 100 nb for masses above 5 GeV/c^2 and charges $q \geqslant 1$) should be made with some caution, since these experiments were performed at different production angles and momenta and used different production models for the calculation of the total cross sections.

We would like to express our thanks to the Experimental Support Group of the ISR division for their continued assistance to this experiment. This work was supported in part by the Stichting voor Fundamenteel Onderzoek der Materie (FOM), which is supported by the Nederlandse Organisatie voor Zuiver Wetenschappelijk Onderzoek (ZWO) and in part by the UK Science Research Council through the Daresbury Laboratory.

References

[1] J.V. Allaby et al., Nuovo Cimento 64A (1969) 75.
[2] T. Massam, The quark hunters progress, CERN report 68–24 (1968).

[3] Y.M. Antipov et al., Phys. Letters 29B (1969) 245; Nucl. Phys. B27 (1971) 374.
[4] L.B. Leipuner et al., Phys. Rev. Letters 31 (1973) 1226.
[5] J.A. Appel et al., Phys. Rev. Letters 32 (1974) 428.
[6] Single Arm Spectrometer Facility Group; Preprint NAL-73/83-Exp, 7100.096 (1973).
[7] M. Bott-Bodenhausen et al., Phys. Letters 40B (1972) 693.
[8] B. Alper et al., Phys. Letters 46B (1973) 265.
[9] J.V. Javanovich et al., Phys. Letters 56B (1975) 105.
[10] D. Amati et al., Phys. Letters 11 (1964) 190.
[11] B.J. Bjorken and S.L. Glashow, Phys. Letters 11 (1964) 255.
[12] S.L. Glashow, J. Iliopoulos and L. Maiani, Phys. Rev. D2 (1970) 1285.
[13] M.Y. Han and Y. Nambu, Phys. Rev. 139B (1965) 1006.
[14] M.G. Albrow et al., Phys. Letters 42B (1972) 279.
[15] M.G. Albrow et al., Nucl. Phys. B54 (1973) 6; B72 (1974) 376.
[16] V.T. Cocconi et al., Phys. Rev. Letters 5 (1960) 19.
[17] W.F. Baker et al., Phys. Rev. Letters 7 (1961) 101.
[18] V.L. Fitch et al., Phys. Rev. 126 (1962) 1849.
[19] A. Schwarzschild and Č. Zupančič, Phys. Rev. 129 (1963) 854.
[20] A.N. Diddens et al., Nuovo Cimento 31 (1964) 961.
[21] J.V. Allaby et al., Phys. Letters 29B (1969) 198.
[22] D.E. Dorfan et al., Phys. Rev. Letters 14 (1965) 1003.
[23] B. Alper et al., Phys. Letters 47B (1973) 275.
[24] P. Capiluppi et al., Nucl. Phys. B79 (1974) 189.
[25] J.V. Allaby et al., CERN-Rome Collaboration report at the Fourth Int. Conf. on high-energy collisions, Oxford (1972).
[26] H. Grote, R. Hagedorn and J. Ranft, Atlas of particle production spectra, Geneva 1970.
[27] T. Massam et al., Nuovo Cimento 39 (1965) 10.
[28] F. Binon et al., Phys. Letters 30B (1969) 510.
[29] Y.M. Antipov et al., Phys. Letters 34B (1971) 164.
[30] M.G. Albrow et al , Nucl. Phys. B73 (1974) 40.